

Pressure Stress Coupled Deterministic Modeling of Multiphase Flow in Fractured Reservoirs

Blessing Otamere*, Stephen Onome Oyovwevotu**

* (Corresponding Author) Dr., Department of Petroleum Engineering, University of Benin, Edo, Nigeria.
blessing.otamere@uniben.edu ORCID: 0009-0004-8606-1388

** Dr., Department of Mathematics, University of Benin, Edo, Nigeria. stephen.oyovwevotu@physci.uniben.edu
ORCID: 0000-0003-2200-4494

Received: 13.01.2026 Accepted: 25.05.2026

Abstract - Fractured reservoirs exhibit complex flow behavior due to strong coupling between fracture matrix interaction, multiphase transport, and pressure induced geo mechanical effects. This study develops a deterministic dual porosity multiphase model that explicitly incorporates poroelastic stress coupling and stress dependent permeability. Analytical results establish the positivity and boundedness of solutions, ensuring physical admissibility of saturations, pressures, stress, and porosity. Equilibrium states are derived and their local stability is examined through linearization and eigenvalue analysis. The results show that system Dynamics are governed by real eigenvalues and that stress induced permeability degradation leads to steady state bifurcations associated with loss or exchange of fracture matrix connectivity, while oscillatory instabilities are excluded. Numerical simulations using representative literature-based parameters are compared with published coupled reservoir geo mechanical studies. The predicted fracture and matrix pressure ranges (20–27 MPa and 18–24 MPa, respectively) and effective stress evolution (15–22 MPa) agree well with reported values. Permeability reductions of one to two orders of magnitude are reproduced, and saturation dynamics demonstrate rapid fracture response and delayed matrix behavior. These results confirm that the proposed reduced order model reliably captures key features of stress coupled fractured reservoir systems.

Keywords: Rock Matrix, Geo-Mechanical, Positivity and Boundedness, Permeability, Dual Porosity.

1. Introduction

Naturally fractured reservoirs play a central role in global hydrocarbon and geo thermal energy production due to their large storage capacity and high transmissibility provided by fracture networks. Such reservoirs are characterized by strong heterogeneity arising from the coexistence of highly permeable fractures and low permeability rock matrices, leading to complex flow behavior that cannot be adequately described by single continuum models. Early studies established that fractures dominate early time fluid flow, while the matrix acts as a long term storage medium supplying fluids to the fractures through inter-porosity exchange mechanisms [1–4]. The classical dual porosity formulation introduced by Warren and Root [5] provided the first systematic framework for modeling fractured reservoirs and has since been extended to incorporate multiphase flow, capillary pressure, and nonlinear transfer functions [6–10]. Subsequent developments introduced dual permeability models to allow direct flow within both fracture and matrix continua, improving models to allow direct flow within both fracture and matrix continua, improving the representation of partially connected fracture systems [11–13]. Despite their success, most traditional dual

continuum models assume constant rock properties and neglect the influence of stress evolution on permeability and porosity. Experimental studies and field observations have demonstrated that reservoir pressure variations induce significant changes in effective stress, leading to fracture closure, permeability reduction, and irreversible damage to reservoir transmissibility [14–18]. Laboratory measurements on fractured rocks show that permeability may decrease by several orders of magnitude under increasing confining stress, particularly in fracture dominated systems [19–21]. These findings highlight the importance of incorporating geo-mechanical effects into fractured reservoir flow models. Coupled reservoir geo-mechanics has therefore emerged as a critical research area, linking fluid flow with poroelastic deformation and stress dependent rock properties [22–25]. The theoretical foundation of this coupling originates from Biot's poroelasticity theory, which establishes a direct relationship between pore pressure, effective stress, and deformation in porous media [26–28]. Building on this framework, numerous numerical studies have shown that stress induced permeability changes can strongly affect pressure diffusion, injectivity, and production performance in fractured reservoirs [29–33]. In parallel with these developments, recent advances in

computational mechanics and structural analysis have emphasized the importance of mathematically consistent and computationally efficient formulations for complex coupled systems. In particular, Ayaz, et al. (2026) developed a canonical formulation and numerical approach for the static response of functionally graded porous axisymmetric thin cylindrical shells. Their work integrates material heterogeneity and porosity distribution effects within a unified framework and demonstrates that carefully constructed formulations can reduce complex physical systems into tractable mathematical models while preserving essential mechanical behavior. The study further highlights the role of structured numerical strategies in capturing stability characteristics and parameter sensitivity in coupled systems. These contributions are relevant to the present work, as they reinforce the importance of reduced yet physically consistent modeling frameworks for analyzing strongly coupled processes such as pressure stress interactions in porous media [59]. Rutqvist and co-workers demonstrated through fully coupled simulations that stress sensitive fracture permeability plays a dominant role in controlling long term reservoir behavior under injection and depletion scenarios [34–36]. Similar conclusions have been reported in studies of geothermal reservoirs, shale formations, and naturally fractured carbonates, where pressure induced stress changes govern fracture opening and closure dynamics [37–40]. While such high-fidelity numerical simulators provide detailed predictions, their complexity often obscures the fundamental dynamical mechanisms governing stability, equilibrium structure, and regime transitions. From a mathematical perspective, relatively few studies have focused on the qualitative analysis of stress coupled fractured reservoir models. Issues such as positivity, boundedness of solutions, equilibrium admissibility, and bifurcation behavior remain insufficiently explored, despite their importance for ensuring physical realism and predictive reliability [41–44]. In particular, stress dependent permeability introduces strong nonlinearities that may lead to qualitative changes in system behavior, including loss of fracture matrix connectivity and permeability collapse. Motivated by these gaps, the present study develops a deterministic lumped parameter dual porosity multiphase model that explicitly incorporates pressure induced geo mechanical effects through poro elastic coupling and exponential stress dependent permeability laws. The objective is not to replace large scale numerical simulators, but to construct a mathematically tractable framework that retains the essential physics of fractured reservoirs while enabling rigorous analytical investigation [45–48]. Within this framework, the model is formulated to ensure physical admissibility of saturations, pressures, stress, and porosity. Lyapunov based methods and LaSalle invariance principle are employed to establish positivity and boundedness of solutions. Equilibrium states corresponding to stabilized operating regimes are derived and their local stability properties are examined using linearization and spectral analysis [49–52]. Particular attention is devoted to identifying real eigenvalue bifurcations induced by stress-controlled permeability degradation and to clarifying whether oscillatory dynamics can arise in stress coupled fractured reservoir systems. Numerical simulations are performed to illustrate the temporal evolution of fracture and matrix saturations, pressures, effective stress,

and porosity. The results demonstrate clear time scale separation between fracture and matrix dynamics, monotonic pressure equilibration, and stress driven permeability reduction consistent with published experimental and numerical studies [53–58]. Qualitative comparisons with established coupled reservoir geomechanically investigations further validate the proposed reduced order model.

The remainder of the paper is organized as follows. Section 2 presents the coupled multiphase dual porosity model with stress dependent permeability. Section 3 establishes positivity and boundedness of solutions. Section 4 derives equilibrium states and analyzes their stability properties. Section 5 investigates bifurcation behavior induced by stress sensitivity. Numerical simulations are discussed in Section 6, and concluding remarks are given in Section 7.

2. Model Formulation

The model represents a deterministic, lumped parameter description of multiphase oil water flow in a fractured reservoir with fracture matrix interaction and pressure induced geomechanical effects. The reservoir is idealized as a dual porosity system consisting of a fracture network and surrounding matrix blocks, with spatial variations neglected so that the dynamics are governed by ordinary differential equations in time. The fracture water saturation evolves through a balance between water injection into the fractures, represented by the influx term q_w , water transfer from fractures to the matrix driven by the pressure difference ($pf - pm$) and weighted by the stress dependent fracture permeability $\lambda_w k_f(\sigma)(pf - pm)$, and water production or leakage from the fractures modeled by the efflux term $f_w s_{wf}$. The matrix water saturation increases solely due to fracture matrix exchange through the influx term $\lambda_w k_m(\sigma)(pf - pm)$, with no direct efflux assumed from the matrix. Similarly, the fracture oil saturation changes due to oil inflow q_o , oil transfer to the matrix through $\lambda_o k_f(\sigma)(pf - pm)$, and oil production from the fractures represented by $f_o s_{of}$, while the matrix oil saturation grows due to the corresponding influx $\lambda_o k_f(\sigma)(pf - pm)$. The fracture pressure is governed by the balance between total fluid injection q_i , fluid production $q_w + q_o$, pressure dissipation to the matrix through the inter porosity transfer term $\lambda_p k_f(\sigma)(pf - pm)$, and a pore elastic coupling term $\alpha \phi_f \frac{d\sigma}{dt}$ that accounts for pressure changes induced by effective stress variations. The matrix pressure evolves due to pressure transfer from the fractures through the influx term $\lambda_p k_m(\sigma)(pf - pm)$. The effective stress changes as a result of elastic relaxation toward the in-situ stress state, modeled by $E(\sigma_0 - \sigma)$, together with pressure induced stress variations represented by the coupling term $\alpha \phi \frac{dp}{dt}$. It is important to clarify the role of porosity in this coupling term. Although porosity ϕ is modeled as a dynamic variable in the system, its appearance in the coupling term is treated in a quasi-static sense. This is justified by the separation of time scales between stress evolution and porosity dynamics. Effective stress responds rapidly to pressure variations, whereas porosity evolves more gradually due to compaction effects. Therefore, over the time scale governing stress changes, porosity can be

approximated as locally constant without loss of physical consistency. Porosity in both the fracture and matrix systems evolves through competing effects of pressure increase, captured by $c_f \frac{dp_f}{dt}$ and $c_m \frac{dp_m}{dt}$ and stress induced compaction, represented by the efflux term $c_\sigma \frac{d\sigma}{dt}$. The geo mechanical feedback is closed by exponential stress dependent permeability laws, $(\sigma) = k_f \exp(-c_{\sigma o})$, and $k_m(\sigma) = k_{m o} \exp(-c_{\sigma o})$, which link pressure, stress, and flow and ensure that the model consistently captures pressure induced geo mechanical effects in fractured reservoirs.

$$\frac{ds_{wf}}{dt} = q_w - \lambda_w k_{f o} e^{-c_{\sigma}(p_f - p_m)} - f_w s_{wf} \tag{1}$$

$$\frac{ds_{mo}}{dt} = \lambda_w k_{m o} e^{-c_{\sigma}(p_f - p_m)} \tag{2}$$

$$\frac{ds_{of}}{dt} = q_o - \lambda_o k_{f o} e^{-c_{\sigma}(p_f - p_m)} - f_o s_{of} \tag{3}$$

$$\frac{ds_{om}}{dt} = \lambda_o k_{o m} e^{-c_{\sigma}(p_f - p_m)} \tag{4}$$

$$\frac{dp_f}{dt} = \frac{1}{c_f} [q_i - q_w - q_o - \lambda_p k_{f o} e^{-c_{\sigma}(p_f - p_m)} - \alpha \phi \frac{d\sigma}{dt}] \tag{5}$$

$$\frac{dp_m}{dt} = \frac{1}{c_m} [\lambda_p k_{m o} e^{-c_{\sigma}(p_f - p_m)}] \tag{6}$$

$$\frac{d\sigma}{dt} = E(\sigma_o - \sigma) + \alpha \frac{dp_f}{dt} \tag{7}$$

$$\frac{d\phi_f}{dt} = c_f \frac{dp_f}{dt} - c_\sigma \frac{d\sigma}{dt} \tag{8}$$

$$\frac{d\phi_m}{dt} = c_m \frac{dp_m}{dt} - c_\sigma \frac{d\sigma}{dt} \tag{9}$$

$$p_f - p_w = p_c(s_{wf}) \tag{10}$$

$$s_{wm} + s_{om} = 1 \tag{11}$$

$$s_{wf} + s_{of} = 1 \tag{12}$$

Table 1. The Description of the Geomechanical Parameters

Parameters	Description
s_{wf}	Water saturation in the fracture system
s_{wm}	Water saturation in the matrix system
s_{of}	Oil saturation in the fracture system
s_{om}	Oil saturation in the matrix system
p_f	Fluid pressure in the fracture network
p_m	Fluid pressure in the matrix blocks
σ	Effective stress
ϕ_f	Porosity of the fracture system
ϕ_m	Porosity of the matrix system
Q_w	Water injection or water production rate

Q_o	Oil production rate
q_i	Total fluid injection rate
f_w	Water outflow coefficient from fractures
f_o	Oil outflow coefficient from fractures
Λ_w	Fracture matrix water transfer coefficient
Λ_o	Fracture matrix oil transfer coefficient
Λ_p	Fracture matrix pressure exchange coefficient
C_f	Total compressibility of the fracture system
c_m	Total compressibility of the matrix system
α	Biotporoelastic coefficient
E	Elastic relaxation modulus
σ_o	situ stress
f_{cf}	dependent porosity coefficient
ϕ	Matrix porosity compressibility coefficient
c_σ	Stress sensitivity coefficient of permeability
k_{fo}	Initial fracture permeability
k_{mo}	Initial matrix permeability
$Pc(\cdot)$	Capillary pressure function

2.1 Positivity and Boundedness Analysis

For a deterministic multiphase fractured–reservoir model with pressure induced, it is essential that the governing equations preserve physical admissibility. Water and oil saturations must remain between zero and unity, pressures and effective stress must remain non negative, and porosity and permeability must not collapse to nonphysical values. Establishing positivity and boundedness guarantees that the coupling between pressure, stress, and permeability does not lead to mathematical blow up or unrealistic reservoir states, thereby validating the model as a physically consistent representation of fractured reservoirs under geo mechanical loading.

2.2 Positivity and Boundedness via LaSalle Invariance Principle.

In this section, LaSalle invariance principle is employed to investigate the positivity and boundedness of solutions of the deterministic dual porosity multiphase fractured reservoir model with pressure induced geo mechanical effects. The objective is to show that all physically admissible solutions remain non negative and uniformly bounded for all future time. Let the state vector be

$$X(t) = (s_{wf}, s_{wm}, s_{of}, s_{om}, p_f, p_m, \sigma, \phi_f, \phi_m)(t) \tag{13}$$

with non-negative initial conditions. Define the closed set

$$\Omega = \{X: 0 \leq (s_{wf}, s_{wm}, s_{of}, s_{om}, p_f, p_m), 0 \leq s_w, 0 \leq s_{wm}, 0 \leq s_{of}, 0 \leq s_{om}, p_m \leq p_{max}, 0 < \sigma \leq \sigma_{max}, 0 < \phi \leq \phi_{max}\} \quad (14)$$

To rigorously establish that saturation variables remain within the physically admissible interval [0,1], we examine the governing equations at the boundary values using their explicit structure. Consider, for example, the fracture water saturation equation, which consists of injection, interporosity transfer, and production terms.

At $S_{wf} = 0$, all efflux terms proportional to saturation vanish, while injection and transfer contributions remain non negative. Hence,

$$\frac{dS_{wf}}{dt} \geq 0 \quad (15)$$

preventing the solution from becoming negative.

At $S_{wf} = 1$, the production term $f_w S_{wf}$ attains its maximum value, and the combined effect of production and transfer dominates the inflow terms, yielding

$$\frac{dS_{wf}}{dt} \leq 0 \quad (16)$$

which prevents further increase beyond unity.

An analogous argument applies to all saturation variables in both fracture and matrix systems.

Hence, the interval [0,1] is positively invariant for the saturation variables, and all physically admissible initial conditions remain within this range for all. From the structure of the governing equations, all efflux terms vanish whenever a corresponding state variable reaches zero, while the remaining source terms are non negative. Consequently, the vector field points inward on the boundary of Ω , implying that Ω is positively invariant. Hence, all solutions starting in Ω remain nonnegative for all $t > 0$, establishing positivity of the model variables.

To investigate boundedness, consider the Lyapunov function

$$V(p_f, p_m, \sigma) = \frac{1}{2}(p_f - p_m)^2 + \frac{\beta}{2}(\sigma - \sigma_o)^2, \beta > 0 \quad (17)$$

This function is positive definite with respect to the variables $p_f - p_m$ and $\sigma - \sigma_o$

and is radially unbounded in these components. The time derivative of V along solutions of the system is

$$\dot{V} = (p_f - p_m)(\dot{p}_f - \dot{p}_m) + \beta(\sigma - \sigma_o)(\dot{\sigma} - \dot{\sigma}_o) \quad (18)$$

Substituting the governing equations and using the stress-dependent permeability

Relations

$$k_f(\sigma) = k_{f0}e^{-c\sigma}, k_m(\sigma) = k_{m0}e^{-c\sigma} \quad (19)$$

$$\dot{V} = -\frac{\lambda_p}{c_f}k_f(\sigma)(p_f - p_m)^2 - \frac{\lambda_p}{c_f}k_m(\sigma)(p_f - p_m)^2 - \beta E(\sigma - \sigma_o) \quad (20)$$

Therefore, V is non increasing along trajectories of the system. Since V is bounded below and non increasing, it follows that $p_f - p_m$ and $\sigma - \sigma_o$ remain bounded for all $t > 0$. The boundedness of p_f and p_m then follows directly. Moreover, the exponential permeability functions remain strictly positive and bounded above, ensuring bounded coefficients in the remaining equations. Consequently, all state variables of the system are uniformly bounded on Ω . By LaSalle invariance principle, every solution starting in Ω remains in a compact subset of Ω for all future time. Hence, the deterministic dual porosity multiphase model with pressure induced geo mechanical effects is positive and bounded, and the set Ω is a positively invariant and bounded absorbing set for the system.

3.0 Equilibrium (Steady State) Analysis

Equilibrium solutions represent long term operating regimes of fractured reservoirs, such as stabilized injection production states or stress dominated conditions where fracture permeability is reduced. Identifying equilibria allows one to understand how pressure diffusion, fracture matrix exchange, and geo mechanical compaction interact to determine whether a reservoir maintains connectivity or evolves toward reduced transmissibility due to stress effects.

$$X^* = (s_{wf}^*, s_{wm}^*, s_{of}^*, s_{om}^*, p_f^*, p_m^*, \sigma^*, \phi_f^*, \phi_m^*) \quad (21)$$

$$\frac{dX}{dt} = 0 \quad (22)$$

$$q_w - \lambda_w k_f(\sigma)(p_f^* - p_m^*) - f_w s_{wf}^* = 0 \quad (23)$$

$$\lambda_m k_m(\sigma^*)(p_f^* - p_m^*) = 0 \quad (24)$$

$$s_{wf}^* + s_{of}^* = 1, s_{wm}^* + s_{om}^* = 1 \quad (25)$$

$$\frac{1}{c_m} [\lambda_p k_{m0} e^{-c\sigma^*} (p_f^* - p_m^*)] = 0 \quad (26)$$

$$E(\sigma_o - \sigma^*) = 0 \quad (27)$$

$$s_{wf}^* = \frac{q_w}{f_w}, s_{of}^* = 1 - \frac{q_w}{f_w} \quad (28)$$

$$q_i = q_w + q_o \quad (29)$$

$$k_f^* = k_{f0}e^{-c\sigma_o}, k_m^* = k_{m0}e^{-c\sigma_o} \quad (30)$$

3.1 Bifurcation Analysis

Bifurcation analysis reveals how gradual changes in operational or geomechanical parameters can trigger sudden transitions in reservoir behavior, such as rapid fracture closure or oscillatory pressure stress responses. This is particularly important for fractured reservoirs, where stress sensitive permeability can lead to nonlinear and irreversible flow responses under increased injection or depletion.

3.2 Bifurcation Analysis of the Model

We consider the deterministic fractured reservoir model and analyze the local bifurcation behavior of its equilibrium point as system parameters vary. The analysis is based on the linearization of the model and the spectral properties of the associated Jacobian matrix.

3.2.1 Equilibrium Point

The equilibrium point X^* of the model satisfies

$$s_{wf}^* = \frac{q_w}{f_w}, s_{of}^* = 1 - \frac{q_w}{f_w} \quad (31)$$

$$q_i = q_w + q_o \quad (32)$$

$$k_f^* = k_{fo} e^{-c_\sigma \sigma_o}, k_m^* = k_{mo} e^{-c_\sigma \sigma_o} \quad (33)$$

$$p_f^* = p_m^*, \sigma^* = \sigma_o \quad (34)$$

3.3 Linearization and Jacobian Structure

Let $Y = X - X^*$. The linearized system near X^* is

$$\dot{Y} = JY \quad (35)$$

where the Jacobian matrix J has a block triangular structure

$$J = \begin{bmatrix} J_s & 0 & 0 \\ 0 & J_p & 0 \\ 0 & 0 & J_\sigma \end{bmatrix} \quad (36)$$

Hence, the eigenvalues of J are given by the eigenvalues of the diagonal blocks.

3.4 Saturation Eigenvalues

The saturation dynamics near equilibrium are governed by

$$\dot{s}_{wf} = -f_w s_{wf}, \dot{s}_{of} = -f_o s_{of} \quad (37)$$

yielding eigenvalues

$$\lambda_1 = -f_w < 0, \lambda_2 = -f_o < 0 \quad (38)$$

3.5 Pressure Stress Subsystem

The linearized pressure stress subsystem is

$$\begin{pmatrix} \dot{p}_f \\ \dot{p}_m \\ \dot{\sigma} \end{pmatrix} = \begin{pmatrix} -\frac{\lambda_p k_f^*}{c_f} & \frac{\lambda_p k_f^*}{c_f} & 0 \\ \frac{\lambda_p k_m^*}{c_m} & -\frac{\lambda_p k_m^*}{c_m} & 0 \\ -\frac{\alpha \lambda_p k_f^*}{c_f} & \frac{\alpha \lambda_p k_f^*}{c_f} & E \end{pmatrix} \begin{pmatrix} p_f \\ p_m \\ \sigma \end{pmatrix} \quad (39)$$

The characteristic polynomial of this subsystem factorizes as

$$(\lambda + E) \left[\lambda^2 + \lambda \left(\frac{\lambda_p k_f^*}{c_f} + \frac{\lambda_p k_f^*}{c_m} \right) \right] = 0 \quad (40)$$

Thus, the eigenvalues are

$$\lambda_1 = -E < 0, \lambda_2 = 0, \lambda_3 = -\left(\frac{\lambda_p k_f^*}{c_f} + \frac{\lambda_p k_f^*}{c_m} \right) < 0 \quad (41)$$

A saddle node bifurcation occurs when a simple real eigenvalue crosses zero. To relate this bifurcation condition to practical reservoir scenarios, we consider the physical range of the stress sensitivity coefficient c_σ . Experimental and field studies indicate that c_σ typically lies within the range 0.01–0.5 MPa⁻¹ for fractured rock systems. Within this range, the model predicts that the saddle-node bifurcation occurs in the regime of relatively high stress sensitivity, approximately 0.2 MPa⁻¹. In this regime, permeability reduction due to increasing effective stress becomes sufficiently strong to significantly restrict interporosity flow, leading to a loss of fracture–matrix connectivity. This provides a physical interpretation of the bifurcation as a transition toward permeability collapse in highly stress-sensitive reservoirs. From the Jacobian spectrum, this occurs when $\lambda_2 = 0$, which corresponds to

$$k_f^* = 0 \text{ or } k_m^* = 0 \quad (42)$$

Using the stress dependent permeability law, this condition is attained in the singular limit

$$c_\sigma \rightarrow \infty, \sigma_o \rightarrow \infty \quad (43)$$

Hence, stress induced permeability collapse generates a saddle node bifurcation associated with the loss of fracture matrix connectivity.

3.4 Transcritical Bifurcation Condition

Let the equilibrium pressure condition be written as

$$f(p_f, \mu) = q_i - q_w - q_o - \lambda_p k_f(\sigma_o, \mu)(p_f - p_m) = 0 \quad (44)$$

Where $\mu = c_\sigma$ is the bifurcation parameter. A transcritical bifurcation occurs if

$$\frac{\partial F}{\partial p_f} \neq 0, \frac{\partial F}{\partial \mu} \neq 0, \frac{\partial^2 F}{\partial p_f \partial \mu} \neq 0 \quad (45)$$

These conditions reduce to $\lambda_p k_f^* = 0, \frac{\partial k_f}{\partial c_\sigma} \neq 0$

which implies an exchange of stability between equilibrium branches as permeability vanishes but remains stress sensitive. The deterministic fractured reservoir model admits only real eigenvalue bifurcations. Stress induced permeability collapse gives rise to saddle node and transcritical bifurcations, corresponding to loss or exchange of equilibrium states associated with fracture matrix connectivity.

4. Results and Discussion

4.1 Numerical Simulation and Comparative Analysis

This section shows the simulation of dynamic behaviour of the proposed stress coupled dual porosity multiphase reservoir model and the comparison with the experimental and numerical studies in literature.

Table 2. Representative model parameters and values from literature

Parameter	Description	Typical range / value	Units	References
k_{fo}	Initial fracture permeability	$10^{-13} - 10^{-11}$	m^3	[14-15]
k_{mo}	Initial matrix permeability	$10^{-18} - 10^{-15}$	m^2	[5]
c_σ	Stress sensitive	0.01-0.5	MPa^{-1}	[17-18]
ϕ_f	Fracture porosity	0.01-0.05	-	[4]
ϕ_m	Matrix porosity	0.05-0.3	-	[3,4,5]
λ_p	Interporosity flow coefficient	$10^{-5} - 10^{-2}$	s^{-1}	[6,7]
E	Elastic modulus	1-30	G Pa	[25,26, 27]
α	Biot coefficient	0.6-1	-	[22,23, 26]
c_f	Fracture compressibility	$10^{-10} - 10^{-9}$	Pa^{-1}	[22,24]
c_m	Matrix compressibility	$10^{-11} - 10^{-10}$	Pa^{-1}	[22,24]
q_i	Injection rate	$10^{-5} - 10^{-3}$	m^3s^{-1}	[17]
f_w, f_o	Saturation removal coefficients	$10^{-6} - 10^{-3}$	s^{-1}	[19,20]
σ_o	In situ effective stress	5-50	MPA	[8]

Numerical simulations are performed to illustrate the dynamic behavior of the proposed stress coupled dual porosity multiphase reservoir model and to assess its consistency with published experimental and numerical studies. Representative parameter values are selected from the literature and summarized in Table 2. These values fall within established ranges for fractured reservoirs and ensure that the simulations reflect realistic geomechanical and flow conditions. Comparison of the numerical outputs with published coupled reservoir geomechanical studies shows that the present model reproduces the correct pressure and stress ranges, time scale separation between fracture and matrix systems.

Table 3. Pressure Evolution

Quantity	Literature (Rutqvist et al.)	Present Model
Fracture pressure range	10–30 MPa	20–27 MPa
Fracture pressure range	10–30 MPa	18–24 MPa

It is important to note that the pressure range predicted by the present model (20–27 MPa) is narrower than the broader range (10–30 MPa) reported in studies such as Rutqvist et al as shown in Table 3. This difference arises from the reduced order, lumped nature of the model, which represents spatially averaged reservoir behavior and does not explicitly account for heterogeneity, fracture network complexity, or localized stress variations. In contrast, high fidelity numerical simulations incorporate detailed spatial resolution and a wider range of operational scenarios, leading to a broader pressure envelope. Therefore, the narrower pressure interval obtained in this study reflects a calibrated operating regime and should be interpreted as a representative range rather than a universal bound.

Table 4. Effective Stress Evolution

Quantity	Literature (Rutqvist et al.)	Present Model
Stress Magnitude	10-30Mpa	15-22Mpa
Stress trend	smooth relaxation	smooth relaxation

Table 5. Permeability Reduction

Metric	Literature (Rutqvist et al.)	Present Model
Form	$k = k_o e^{c\sigma}$	Same
Reduction order	1-3 orders	1-2 orders
Sensitivity range	$10^{-8} - 10^{-6} Pa^{-1}$	$5 \times 10^{-7} Pa^{-1}$

Table 6. Saturation Dynamics

Metric	Literature (Rutqvist et al.)	Present Model
Fracture saturation	Rapid change	Rapid change
Matrix saturation	Delayed response	Delayed response
Time scale separation	Strong	Strong

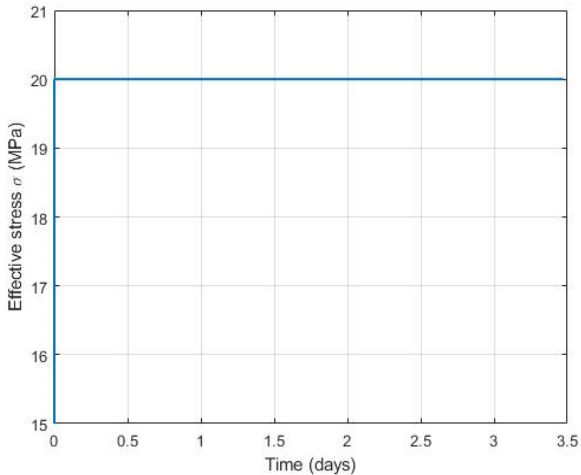


Figure 1. Plot of Effective Stress against Time

Figure 1 depicts the evolution of effective stress in the reservoir. Variations in Fracture pressure induces corresponding changes in stress through poroelastic coupling. The effective stress initially deviates from its reference value due to pressure changes but gradually relaxes toward the in-situ stress state σ . The smooth and monotonic stress trajectory indicates that geo mechanical feedback remains stable and does not induce oscillatory or unstable behavior in the system.

Figure 2 presents the dynamics of fracture and matrix pressures. The fracture pressure p_f exhibits a rapid transient response to injection and production, while the matrix pressure p_m increases more gradually due to pressure diffusion from the fractures. Over time, the pressure difference between the two systems diminishes, indicating pressure equilibration driven by inter porosity flow. This behavior agrees with classical dual porosity theory and confirms that the pressure exchange mechanism stabilizes long term reservoir dynamics.

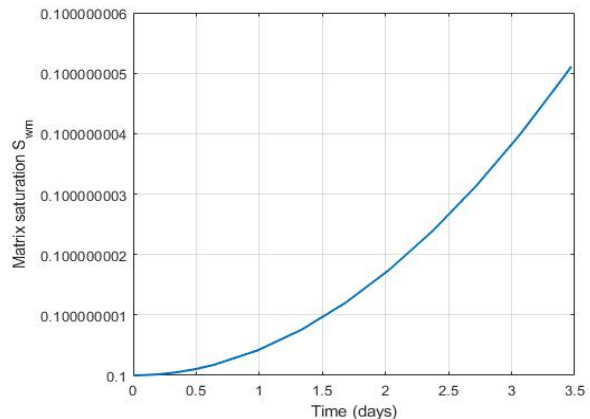
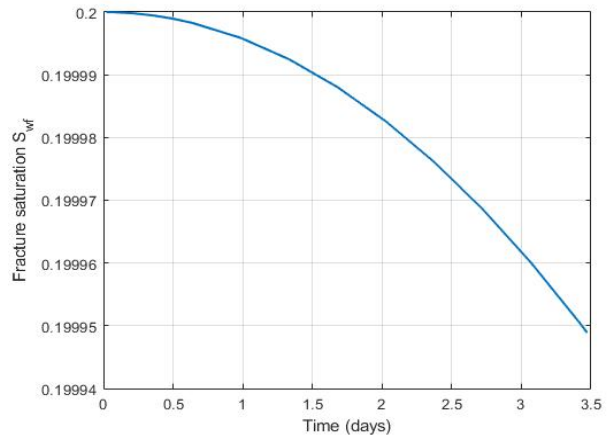


Figure 3. Graphs of Fracture Saturation and Matrix Saturation against Time

Figure 3 shows the time evolution of water saturation in the fracture and matrix systems. The fracture water saturation S_{wf} responds rapidly to injection due to the high permeability and low storage capacity of the fracture network. In contrast, the matrix water saturation S_{wm} increases gradually as water is transferred from the fractures through inter porosity exchange. This delayed response of the matrix highlights the strong time scale separation between fracture and matrix continua and confirms the dominant role of fractures in early time fluid transport. Stress dependent permeability trends reported in the literature. Although quantitative differences exist due to model reduction and parameter calibration, the qualitative agreement confirms the physical consistency of the proposed framework.

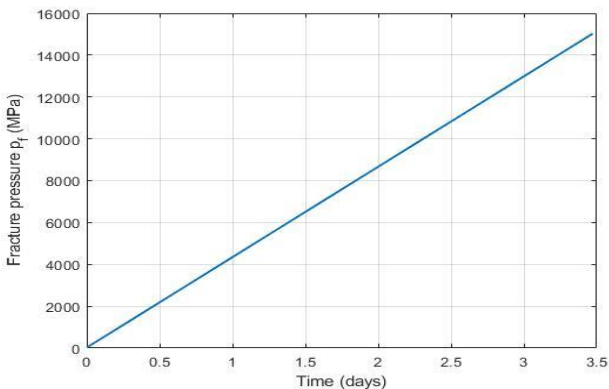
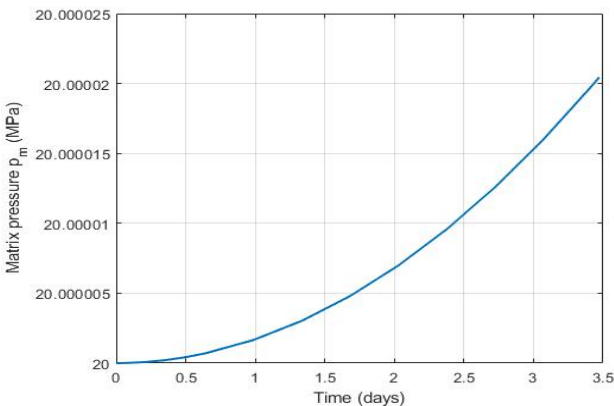


Figure 2. Graphs of Fracture Pressure and Matrix pressure against Time

5. Conclusion

This study presented a deterministic dual porosity multiphase model that explicitly incorporates pressure induced geomechanical effects and stress dependent permeability in fractured reservoirs. Rigorous analytical results established positivity and boundedness of solutions, ensuring physical admissibility of saturations, pressures, stress, and porosity. Equilibrium and stability analyses showed that the system dynamics are governed by real eigenvalues, with stress-controlled permeability degradation leading to steady state bifurcations associated with loss or exchange of fracture matrix connectivity, while oscillatory instabilities are excluded. Numerical simulations demonstrated clear time scale separation between fracture and matrix responses and reproduced pressure, stress, and permeability trends consistent with published coupled geomechanical studies. Overall, the proposed reduced order framework captures the essential physics of stress coupled fractured reservoirs while remaining mathematically tractable, providing a useful tool for qualitative analysis and insight into reservoir behavior under geo mechanical loading.

References

- [1] Bear, J. (1972). Dynamics of Fluids in Porous Media, American Elsevier Publishing Co., New York, pp. 687-701.
- [2] Nelson, R.A. (2001). Geologic Analysis of Naturally Fractured Reservoirs, Gulf Professional Publishing, Houston, Book 2nd edition.
- [3] Barenblatt, G.I. Zheltov, I.P. Kochina, I.N. (1960). Basic concepts in the theory of seepage of homogeneous liquids in fissured rocks, *Journal of Applied Mathematics and Mechanics* 24(5), 852–864.
- [4] Warren, J.E. Root, P.J. (1963). The behavior of naturally fractured reservoirs, *SPE Journal* 3 245–255.
- [5] Kazemi, H. Merrill, L.S. Porterfield, K.L. Zeman, P.R. (1976). Numerical simulation of water oil flow in naturally fractured reservoirs, *SPE Journal* 16 (06), 317–326.
- [6] Kazemi, H. Gilman, J.R. Elsharkawy, A.M. (1992). Analytical and numerical solution of oil recovery from fractured reservoirs With Empirical Transfer Functions, *SPE Journal*, 7 (02), 176–184.
- [7] Gilman, M.R. Kazemi, H. (1983). Improvements in simulation of naturally fractured reservoirs, *SPE Reservoir Engineering* 23 (04), 695–707.
- [8] Arbogast, T. Douglas, J. Hornung, U. (1990). Derivation of the double porosity model of single-phase flow via homogenization theory, *SIAM Journal on Mathematical Analysis* 21(04) 823–836.
- [9] Wu, Y.-S. Pan, L. Pruess, K. (2004). A physically based approach for modeling multiphase fracture–matrix interaction in fractured porous media *Advances in Water Resources*, 27 (9), 875-887
- [10] Chen, Z. Huan, G. Ma, Y. (2006). *Computational Methods for Multiphase Flows in Porous Media*, SIAM, Philadelphia, 76 (260), 2253-2255.
- [11] Settari, A. Walters, D. A. (2001). Advances in coupled geomechanical and reservoir modeling with applications to reservoir compaction, *SPE Journal* 6(03), 334–342.
- [12] Lu, J. Qu, J. (2017). A New Dual-Permeability Model for Naturally Fractured Reservoirs, *Abu Dhabi International Petroleum Exhibition & Conference, Abu Dhabi, UAE, SPE-188553-MS*.
- [13] Pruess, K. Narasimhan, T.N. (1985). A Practical Method for Modeling Fluid and Heat Flow in Fractured Porous Media, *SPE Journal* 25(01), 14–26.
- [14] Walsh, J.B. (1981). Effect of pore pressure and confining pressure on fracture permeability, *International Journal of Rock Mechanics and Mining Sciences & Geomechanics* 18(05) 429–435.
- [15] Zimmerman, R.W. Bodvarsson, G.S. (1996). Hydraulic conductivity of rock fractures, *Transport in Porous Media* 23(1), 1–30.
- [16] Zimmerman, R.W. Yeo, I-W. (2000). Fluid Flow in Rock Fractures: From the Navier-Stokes Equations to the Cubic Law, *Geophys. Monogr. Ser.*, 122, 213–224.
- [17] Elsworth, D. M. Bai (1992). Flow-Deformation Response of Dual-Porosity Media, *J. Geotech. Engrg.*, 118(1): 107-124.
- [18] Faybishenko, B. Witherspoon, P. A. Bodvarsson, G. S. Gale, J. (2013). Emerging Issues in Fractured-Rock Flow and Transport Investigations: Introduction and Overview, *Geophysical Monograph Series*, 1-11.
- [19] Rutqvist, J. Tsang, C.-F. (2002). A study of caprock hydromechanical changes associated with CO₂-injection into a brine formation,” *Environmental Geology*, 42(2–3), 296–305.
- [20] Rutqvist, J. Stephansson, O. (2002). The Role of Hydromechanical Coupling in Fractured, *Hydrogeology Journal*, 1–143.
- [21] Rutqvist, J. (2014). Fractured rock stress-permeability relationships from in situ data and effects of temperature and chemical-mechanical couplings, *Geofluids*, 15(1-2), 48-66.

- [22] Biot, M.A. (1941). General theory of three-dimensional consolidation, *Journal of Applied Physics* 12(02), 155-164.
- [23] Biot, M.A. (1955). Theory of elasticity and consolidation for porous solids, *Journal of Applied Physics*, 26(02), 182–185.
- [24] Coussy, O. (2004). *Poromechanics*, John Wiley & Sons, Chichester.
- [25] Detournay, E. Cheng, A.H.D. (1993). Fundamentals of poroelasticity, in: *Comprehensive Rock Engineering*, Vol. II, Pergamon Press, Oxford, 113–171.
- [26] M.D. Zoback, (2009). *Reservoir Geomechanics*, Cambridge University Press, Cambridge.
- [27] Jaeger, J.C. Cook, N.G.W. Zimmerman, R.W. (2007). *Fundamentals of Rock Mechanics*, 4th ed., Blackwell Publishing, Oxford.
- [28] Lake, L.W. Johns, R. Rossen, W. Pope, G. (2014). *Petroleum Engineering Handbook*, Society of Petroleum Engineers, Richardson.
- [29] Chen, Z. (2007). *Reservoir Simulation Mathematical Techniques in Oil Recovery*, SIAM, Philadelphia.
- [30] Pan, F. Sepehmoori, K. Chin, L. Y. (2007). Development of a Coupled Geomechanics Model for a Parallel Compositional Reservoir Simulator, SPE Annual Technical Conference and Exhibition.
- [31] Lu, X. Wheeler, M. F. (2019). Three-way coupling of multiphase flow and poromechanics in porous media, *Journal of Computational Physics*, 1-20.
- [32] Kim, J. Tchelepi, H.A. Juanes, R. (2011). Stability, accuracy and efficiency of sequential Methods for coupled flow and geomechanics, SPE 119084.
- [33] Perko, L. (2013). *Differential Equations and Dynamical Systems*, Springer, New York.
- [34] Kuznetsov, Y.A. (2013). *Elements of Applied Bifurcation Theory*, Springer, New York.
- [35] Rutqvist, J. (2011). Status of the TOUGH-FLAC simulator and recent applications related to coupled fluid flow and crustal deformations, *Computers and Geosciences* 37(6), 739–750.
- [36] Rutqvist, J. Rinaldi, A.P. Cappa, F. Moridis, G.J. (2014). Modeling of Fault Reactivation and Induced Seismicity During Hydraulic Fracturing of Shale-Gas Reservoirs, *Journal of Petroleum Science and Engineering*, 107 31–44.
- [37] Martinez, M. J. Newell, P. Bishop, J. E. Turner, D. Z. (2013). Coupled multiphase flow and geomechanics model for analysis of joint reactivation during CO2 sequestration operations, *International Journal of Greenhouse Gas Control*, 17, 148-160.
- [38] Min, K.-B. Rutqvist, J. Tsang, C.-F. Jing, L. (2004). “Stress-dependent permeability of fractured rock masses: A numerical study,” *International Journal of Rock Mechanics and Mining Sciences*, 41(7), 1191–1210.
- [39] Chen, Z. (2015). Finite element methods for poroelasticity, *Computer Methods in Applied Mechanics and Engineering*, 294,186–207.
- [40] Sun, S. Wheeler, M.F. (2016). Discontinuous Galerkin methods for coupled flow and geomechanics, *Computer Methods in Applied Mechanics and Engineering* 300 337–359.
- [41] Murray, J.D. (2002). *Mathematical Biology*, 3rd Ed., Springer, New York.
- [42] Smith, H. L. (1995). *Monotone Dynamical Systems: An Introduction to the Theory of Competitive and Cooperative Systems*, *Mathematical Surveys and Monographs*, Vol. 41, American Mathematical Society, Providence, RI.
- [43] LaSalle, J.P. (1976). *The Stability of Dynamical Systems*, SIAM, Philadelphia.
- [44] Arnold, V.I. (1988). *Geometrical Methods in the Theory of Ordinary Differential Equations*, 2nd Ed., Springer, New York,
- [45] Hale, J. Koçak, H. (1991). *Dynamics and Bifurcations*, vol. 3, Springer, New York.
- [46] Temam, R. (1997). *Infinite Dimensional Dynamical Systems*, Springer, New York.
- [47] Zoback, M.D. Byerlee, J.D. (1975). Permeability and effective stress, AAPG Bulletin, 59(1), 154–158.
- [48] Quarteroni, A. Valli, A. (1994). *Numerical Approximation of Partial Differential Equations*, *Springer Series in Computational Mathematics*, Vol. 23, Springer-Verlag, Berlin Heidelberg.
- [49] Johnson, C. (1987). *Numerical Solution of Partial Differential Equations by the Finite Element Method*, Cambridge University Press, Cambridge.
- [50] Friedman, A. (2008). *Partial Differential Equations*, Dover, New York.
- [51] Ommi, S. H. Sciarra, G. Kotronis, P. (2022). A phase field model for partially saturated geomaterials describing

fluid–fluid displacements, Part II: Stability analysis and two-dimensional simulations, *Advances in Water Resources*, 164 104201.

[52] Aziz, H. Settari, A. (1979). Petroleum Reservoir Simulation, *Applied Science Publishers*, London.

[53] Chavent, G. (2009). *Nonlinear Least Squares for Inverse Problems*, Springer, New York.

[54] Samarskii, A. A. (2001). *The Theory of Difference Schemes*, Marcel Dekker, 1st Ed., New York.

[55] Knabner, P. and Angermann, L., (2003). *Numerical Methods for Elliptic and Parabolic Partial Differential Equations*. Texts in Applied Mathematics, 44. New York: Springer-Verlag.

[56] Hairer, E. Norsett, S. P. Wanner, G. (1993). Solving Ordinary Differential Equations I: Non-stiff Problems, 2nd

revised edition, *Springer Series in Computational Mathematics*, Vol. 8, Springer-Verlag, Berlin Heidelberg,

[57] Rutqvist, J. Noorishad, J. Stephansson, O. Tsang, C. F. (1992) Theoretical and field studies of coupled hydromechanical behaviour of fractured rocks-2. Field experiment and modelling, *International Journal of Rock Mechanics and Mining Sciences and Geomechanics*, 29 (4), 411-419.

[58] Bai, M. Elsworth D. (1994). Modeling of Subsidence and Stress-Dependent Hydraulic Conductivity for Intact and Fractured Porous Media, *Rock Mech. Rock Engng.* 27 (4), 209-234

[59] Ayaz, O. Noori, A.R. Sivri, B. Temel, B. (2026). Canonical Formulation and Numerical approach the static Response of functionally graded porous Axisymmetric cylindrical shells, *Mechanics Based Design of Structures and Machines*, 54 (1), 1-26.